Coating stability and insertion forces of an alginate-cell-based drug delivery implant system for the inner ear

Silke Hügl[a,b], Verena Scheper[a,b], Michael M. Gepp[c,d], Thomas Lenarz[a,b], Thomas S. Rau[a,b], Jana Schwieger[a,*]

[a] Hannover Medical School (MHH), Department of Otolaryngology, Carl-Neuberg-Str. 1, 30625, Hannover, Germany
[b] Cluster of Excellence EXC 1077/1 "Hearing4all", Hannover Medical School, Carl-Neuberg-Str. 1, 30625, Hannover, Germany
[c] Fraunhofer-Institute for Biomedical Engineering, Joseph-von-Fraunhofer-Weg 1, 66280, Sulzbach, Germany
[d] Fraunhofer-Project Center for Stem Cell Process Engineering, Neunerplatz 2, 97082, Würzburg, Germany

ARTICLE INFO

ABSTRACT:

Long-term drug delivery to the inner ear for neuroprotection might improve the outcome for hearing disabled patients treated with a cochlear implant (CI). Neurotrophic factor (NTF) producing cells encapsulated in an alginate-matrix, to shield them from the host immune system and to avoid migration, and applied as viscose solution or electrode coating could address this requirement. Both application methods were tested for their feasibility in an artificial human cochlea model. Since both strategies potentially influence the electrode implantability, insertion forces and coating stability were analyzed on custom-made electrode arrays. Both, injection of the alginate-cell solution into the model and a manual dip coating of electrode arrays with subsequent insertion into the model were possible. The insertion forces of coated arrays were reduced by 75% of an uncoated reference. In contrast, filling of the model with non-crosslinked alginate-cell solution slightly increased the insertion forces. A good stability of the coating was observed after first insertion (85%) but abrasion increased after multiple insertions (50%). Both application strategies are possible options for cell-induced drug-delivery to the inner ear, but an alginate-cell coating of CI-electrodes has a great potential to combine an endogenous NTF-source with a strong reduction of insertion forces.

1. Introduction

Worldwide, millions of people suffer from sensorineural hearing loss with negative effects in social, emotional and economic field due to a limited ability of communication (Stevens et al., 2013; Word Health Organization, 2018). Patients with severe to profound hearing loss can receive a cochlear implant (CI). The CI consists of an electrode array which is implanted into the scala tympani of the cochlea for electrical stimulation of the spiral ganglion neurons (SGN) which subsequently leads to sound perception in the patient. In hearing impaired patients the SGN degenerate over time (Glueckert et al., 2005; Nadol et al., 1989). A high number of stimulated neurons is considered to positively influence the outcome of the CI in patients (Landry et al., 2013; Senn et al., 2017; Seyyedi et al., 2014; Shepherd et al., 2005; Shibata et al., 2010).

One approach to keep the number of SGN stable is the application of neurotrophic factors (NTF) like brain-derived neurotrophic factor (BDNF) (e.g. (Glueckert et al., 2008; Pettingill et al., 2011; Roehm and Hansen, 2005; Schwieger et al., 2015)). To maintain the benefits of NTF-treatment on CI-outcome a long-term delivery of the therapeutic factor is likely to be required (Gillespie et al., 2014, 2003; Pettingill et al., 2007; Shepherd et al., 2008). Drug delivery systems like intratympanic injections, round window applications, degradable NTF-eluting coatings, (mini-)osmotic pumps, stem cell or gene therapies of inner ear cells have either the disadvantages of a short-term application of the NTFs, or an increased risk of infections or a potentially uncontrolled spread of cells or genes (for overviews, see (Gillespie et al., 2014; Gillespie and Shepherd, 2005; Liu et al., 2013; Pettingill et al., 2007)). Nevertheless, cell-based drug delivery strategies have a great potential for long-term NTF-treatment of SGN. Cells can be genetically modified to produce NTF (Harper et al., 2011; Sasaki et al., 2009; Zhao et al., 2004) and could be provided to the inner ear beside or in conjunction with the CI during surgery (Konerding et al., 2017; Pettingill et al., 2011; Rejali et al., 2007; Warnecke et al., 2012). To avoid detachment or migration of the cells and to isolate them from the host immune system, they can be encapsulated in an alginate matrix

---

(Skinner et al., 2009).

Ultra high viscosity (UHV) alginate of medical-grade is particularly characterized by a high grade of biocompatibility, stability and flexibility. Ba^{2+}-crosslinking of this hydrogel results in a better long-term mechanical stability (Bajpai and Sharma, 2004; Zimmermann et al., 2007, 2005), whereas the inflammatory response is reduced (De Vos et al., 1997; Schneider et al., 2003; Tam et al., 2011). An implant coating with alginate might provide a mechanical buffer to protect sensible surrounding tissue (Abidian and Martin, 2009; Kim et al., 2010) as well as encapsulated cells (Aguado et al., 2012; Foster et al., 2017). Regenerated neurites may grow through the hydrogel matrix, to close the anatomical gap between neurons and electrode. Additionally, it may act as lubricant for the electrode array to reduce insertion forces (Kontorinis et al., 2011).

To optimize the CI outcome, the surgical approach, the electrode array insertion and the electrode design are also in the focus of R&D to avoid intracochlear trauma (Dhanasingh and Jolly, 2017). An atraumatic insertion protecting the structural integrity of soft and bony intracochlear tissue may decrease the risk for inflammatory reactions (Bas et al., 2012; Lehnhardt, 1993; van de Water et al., 2010) or auditory neuron death, which both could reduce the CI outcome (Bas et al., 2015; Kikkawa et al., 2014) and the preservation of residual hearing (Radeloff et al., 2009; Schendzielorz et al., 2014).

For novel electrode generations the development concentrates on improvement towards thinner and more flexible arrays (Drouillard et al., 2017; Gnansia et al., 2016; Lenarz et al., 2009; Nguyen et al., 2013). Additionally, pharmacological functionalization of the electrode array by drug incorporation or drug-loaded coatings were tested for their anti-fibrotic effects (Bohl et al., 2012; Farhadi et al., 2013; Wilk et al., 2016; Wrzeszcz et al., 2014). An analysis of the mechanical effect of coatings on the insertion process, especially on the insertion forces (Radeloff et al., 2009; Roemer et al., 2016; Wrzeszcz et al., 2015) and the stability of the coating after insertion (Ceschi et al., 2014; Schendzielorz et al., 2014) remained disregarded in most studies.

We propose that a cell-mediated BDNF delivery based on electrode surface modification by UHV-alginate coating can possibly address both improvement strategies – neuroprotection and insertion force reduction – for a better CI outcome. Here we investigated UHV-alginate with encapsulated NTF-producing cells as viscose solution or electrode coating for its impact on insertion forces. Next to this the coating was analysed regarding thickness and stability.

2. Materials and methods

2.1. Electrode array fabrication

Commercial CI electrode arrays are very expensive, which may lead to small sample sizes in experiments. In order to provide a sufficient quantity of samples for insertion experiments, custom-made electrode arrays (intracochlear length 17.2 mm, basal/apical diameter of 0.8/0.5 mm, tip of 0.2 mm diameter) were fabricated (Hügl et al., 2018). Their diameter and intracochlear length are compared to the dimensions of electrode arrays from different manufacturers in Table 1.

Three marker ribs were included as visual indication of completed insertion at the end of the conical, intracochlear part of the electrode array (Fig. 1). A small wing follows after the marker ribs for rotation identification.

For fabrication Sylgard 184 (Dow, Barry, UK), a two-component silicone for room temperature cure, was used. For better visibility of arrays and applied coating during insertion and microscopy the silicone was dyed blue (Silc Pig Blue, Smooth-On Inc., Macungie, USA). Four bare copper wires of graded length were placed inside the casting mould before application of the silicone to mimic a stiffness gradient within the array (Hügl et al., 2018). All fabricated arrays were sterilized by UV-sterilization ($1800 \times 100\,\mu J/cm^2$, 1800 s; XL-1000 UV crosslinker, Spectro Linker™; Biotec-Fischer, Reiskirchen, Germany) as

Table 1

Dimensions of custom-made electrode array in comparison to commercially available straight cochlear implant electrode arrays (Gnansia et al., 2016; Mistrík et al., 2017; Mom et al., 2016; Oticon medical, 2019).

manufacturer	electrode array	basal diameter (mm)	apical diameter (mm)	intracochlear length (mm)
Advanced Bionics	SlimJ	0.56 × 0.79	0.26 × 0.55	23
Cochlear Ltd.	SlimStraight	0.6	0.3	20 - 25
Med-El	Flex Soft	1.3	0.5 × 0.4	31.3
	Flex28	0.8	0.5 × 0.4	28
	Flex24	0.8	0.5 × 0.3	24
	Flex20	0.8	0.5 × 0.3	20
Oticon Medical	Classic	1.07	0.5	26
	Evo	0.5	0.4	25
This study	custom	0.8	0.5	17.2

preparation for a coating with drug delivering cells.

2.2. Drug delivering cells

Human bone marrow derived mesenchymal stem cells (MSCs) were chosen as NTF-source and genetically modified for BDNF-production and fluorescent marker gene expression (kindly provided by Prof. Andrea Hoffmann, Department of Orthopaedic Surgery, Hannover Medical School, Hannover, Germany; approved by the ethical committee of Hannover Medical School, Hannover, Germany, (565–2009, 565–2016)). Cells were maintained under proliferating conditions in culture flasks at 37 °C and 5% CO_2 until used. For the experiments, cells were detached by addition of trypsin/EDTA solution (0.25%; Biochrom) for 5 min at 37 °C and 5% CO_2. Serum-containing medium was used to stop the trypsinization and cells were resuspended. Subsequently the number of viable cells was determined by trypan blue exclusion test (Sigma-Aldrich, Merck KGaA, Darmstadt, Germany) in a Fuchs Rosenthal chamber (Brand, Wertheim, Germany). The cell suspension was transferred to a falcon tube (Greiner, Merck KGaA) and centrifuged for 5 min at 800 rpm to obtain an adherent cell pellet. Supernatant was withdrawn and the cells were resuspended in alginate.

2.3. Alginate-layer formation on electrode-like wires

Platinum/Iridium wires (Sigma Aldrich, Merck KGaA) were cleaned using argon plasma (kINPen®, neoplas tools GmbH, Greifswald, Germany) and pre-coated with poly-L-Lysine (pLL (Sigma Aldrich) 1:10 in phosphate-buffered saline (Invitrogen, Carlsbad, USA)) for at least 30 min. After drying at room temperature, wires were covered stepwise by (1) dipping into alginate solution, (2) gelling with 20 mM $BaCl_2$ cross-linking solution (with 5 mM L-histidine and 115 mM NaCl, all chemicals from Sigma-Aldrich) and (3) rinsing in saline (NaCl 0.9%; B.Braun Melsungen AG, Melsungen, Germany). Diameters of coated wires were measured manually (Fig. 2 A) after each coating step (Nikon Instruments GmbH, NIS-elements image analysis software, Duesseldorf, Germany).

2.4. Coating and embedding of MSC on silicone tubings

The coating of electrodes with alginate and MSCs was simulated and optimized using silicone tubings. In order to enable the preparation of cellularized electrodes immediately before application, the coating procedure was designed with commonly available chemicals and tools. Silicone tubings were treated with pLL-solution without prior plasma treatment. After air-drying the silicone's surface was covered with one layer of UHV-alginate (0.65%, provided by Fraunhofer IBMT, Sulzbach, Germany; now available from Alginatec GmbH, Riedenheim, Germany) with suspended cells (> 250,000 cells/ml alginate) and subsequently cross-linked with 20 mM $BaCl_2$ solution. The silicone tubing was dipped
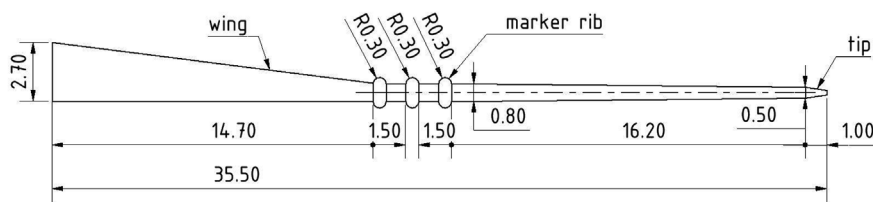
Fig. 1. Schematic drawing of a custom-made electrode array with functional measures in mm.

in an alginate reservoir with suspended cells and covered by a circular movement before gelation. Coated silicone tubings were rinsed carefully with saline and the procedure was repeated two times. Subsequently two protecting alginate layers without cells were applied following the same procedure. Rinsing with saline between the gelation steps was crucial in order to avoid gelation of alginate in the reservoirs. After coating the well separated layers were visible on the silicone tubing (Fig. 2 B). A detailed description of the final coating procedure for human-size custom-made electrode arrays is given in the section "Electrode array coating". The stability of the layered coating and viability of the embedded cells by detection of fluorescent marker gene expression was tested *in vitro* for up to three weeks.

2.5. Alginate encapsulated MSC for cochlea model injection

A cell number of 1.5×10^6 cells/ml was adjusted and cell suspension was added to the UHV-alginate in a ratio of 1:6 for a final cell concentration of 250,000 cells/ml. For this concentration a neuroprotective effect on SGN is verified *in vitro* (Schwieger et al., 2018). The alginate-cell solution was transferred in a 1 ml syringe for application into the artificial cochlea model (aCM).

2.6. Electrode array coating

The custom made electrode arrays were dip-coated in layers with the alginate-cell solution from tip to marker ribs under sterile conditions (Fig. 3). First, arrays were pre-coated with poly-L-Lysine solution (pLL (Sigma Aldrich) 1:10 in Ca^{2+}/Mg^{2+}-free PBS (phosphate-buffered saline) (Invitrogen, Carlsbad, USA)) for 40–50 min, with a subsequent drying step at room temperature. For the inner cell containing layers of the coating a mean of ~400,000 cells (± ~125,000) was embedded in 500 μl alginate as dipping-solution. Each alginate layer was gelled by ionic crosslinking for 20 s and crosslinking agent was washed out by rinsing in saline (NaCl 0.9%; B.Braun Melsungen AG) before next layer was applied. Crosslinking solution was composed of 20 mM $BaCl_2$ (Sigma Aldrich), 115 mM NaCl (Roth, Karlsruhe, Germany) and 5 mM L-histidine (Genaxxo bioscience, Ulm, Germany) and adjusted to a pH of 7 before filtered for sterility (Gepp et al., 2009; Hütten et al., 2013). To apply inner cell-containing alginate layers arrays were dipped four times in the cell solution followed by apply of three outer layers of pure alginate to cover the cell containing inner layers. Each layer formation was monitored under microscopic control. After formation of the last free alginate layer, a final gelation was performed for 5 min with

subsequent photo documentation of each coated array (Fig. 3, A).

2.7. Water contact angle measurement

The surface conditions of an implant can influence the implantation properties and inflammation reactions. For example silicone has the disadvantage of hydrophobicity and a tendency for protein, cell and bacteria adhesion. Therefore, the influence of the coating is tested for its impact on the wettability of silicone. Four different materials were tested by water contact angle measurement. Round disks of silicone without (clear silicone) and with blue dye (dyed silicone) were fabricated from the same two-component silicone material, which was previously used for array fabrication. Mixing of the two components and curing was conducted as described above. A slice of dyed silicone and a cover glass (Ø 30 mm, Menzel GmbH, Braunschweig, Germany) were dip coated with two layers of UHV-alginate as described above. The coated silicone disk and cover glass were stored in saline until tested. Water contact angle measurements were performed and analyzed with the *Surftens Universal and associated software* (OEG, Frankfurt, Germany; kindly provided by AG Behrens, Leibniz University Hannover). Three different positions were tested on each material sample and the contact angle measurements of a deionized water droplet were repeated in triplicate and averaged. Before alginate-coated silicone and cover glass were placed on the device, saline was drained and residual fluids at the edge were carefully dabbed. After 2 min of air drying, measurements were performed. To exclude an influence of possibly remaining sodium chloride crystals on the droplet formation, coated samples were shortly rinsed with deionized water, residual fluid was removed as described before and the contact angle measurements were repeated.

2.8. Experimental groups & insertion setup and procedure

Custom-made electrode arrays were inserted in three different ways (Table 2) into an aCM (Fig. 5) and examined for their insertion forces. Each combination is thereinafter referred to as group, where each group comprised 20 arrays (see Table 2).

To enable standardized and reproducible insertions, an automated insertion test bench was used, which was previously developed and described in detail (Hügl et al., 2018). In short, this setup comprised a linear stage onto which surgical forceps were mounted for gripping and movement of the arrays. They were inserted into a custom-made, planar aCM milled from Polytetrafluoroethylene (PTFE) and covered with
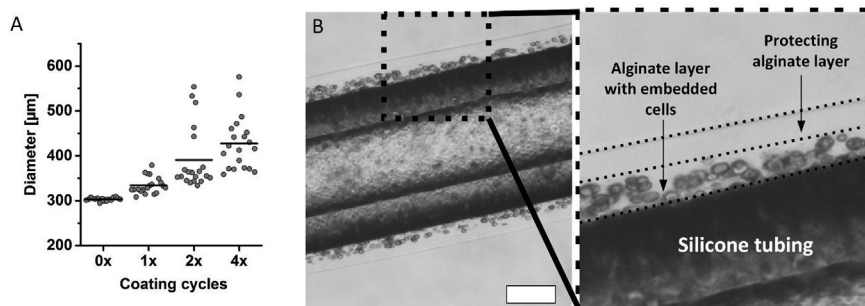

Fig. 2. (**A**) Stepwise coating of Pt–Ir wires with UHV-alginate hydrogel, given as wire diameter plus applied surrounding coating measured after each coating cycle. After repeated cycles a multilayer of alginate of approximately 60 μm is covering the wire's surface. (**B**) Coating of silicone tubings with cells and a protecting alginate layer. The protecting alginate layer avoids release of cells during cultivation and is stable for the tested time period (three weeks). Scale bar in (**B**): 200 μm.
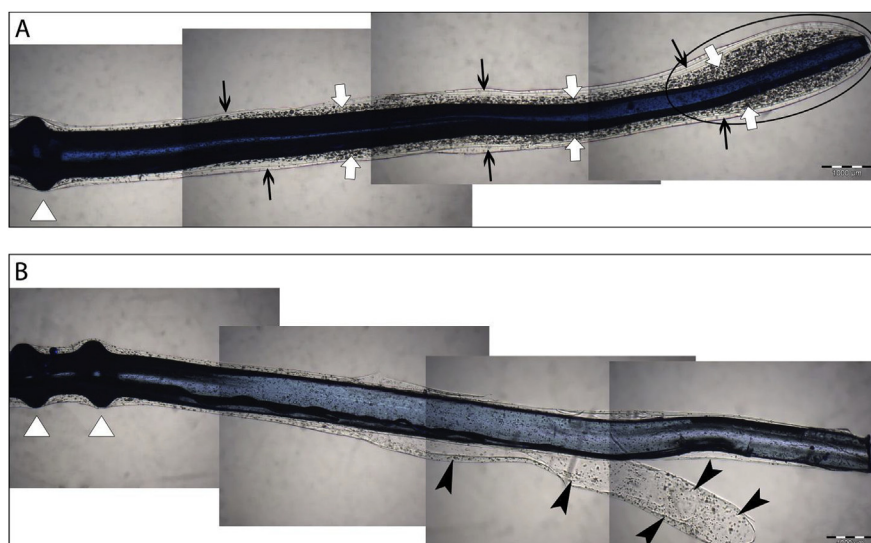
Fig. 3. Coated human-sized custom-made electrode arrays with (**A**) inner cell-containing (spotted, white arrows) and outer cell-free (transparent, black arrows) alginate layers. A droplet formation at the tip with increased coating thickness is often noticeable (circle). Single pictures of the array sections were assembled for evaluation of the whole arrays. (**B**) depicts an example for abrasion with delamination of cell containing coating layers (black arrow heads) scored to grade 5. The images exemplify the contrast enhancement between the transparent alginate layers and the array achieved by blue coloring of the silicone. Triangles point at the marker ribs. Scale bar: 1000 μm.

acrylic glass to enable a direct view of the array during insertion. The aCM was mounted on a force sensor (K3D35, ME-Meßsysteme GmbH, Hennigsdorf, Germany; 0.5 N nominal force, accuracy class 2%) and aligned to the movement axis of the linear stage. A microscopic camera was used for documentation of the insertion procedure. The linear stage and the force sensor were connected to a personal computer on which a custom-made software (developed using C++; Visual Studio, 2015; Microsoft Corporation, Redmond, Washington, USA) was run for insertion controlling and force measurement.

A total of 60 electrode arrays were used in three groups (Table 2): Each array was inserted three times, resulting in 60 insertions for each group. Reproducible insertion forces with repeated insertion of one array were checked previously (Hügl et al., 2018).

Calibration of the force sensor was verified before a new group of arrays was inserted (5 g and 20 g, class M1 knob weights, Häfner Gewichte GmbH, Oberrot, Germany). Afterwards the acrylic disk was mounted on the PTFE-base of the aCM and the cavity was filled with saline (Kontorinis et al., 2012; Leon et al., 2018; Nguyen et al., 2012). Arrays of the reference group (group 1) were gripped at marker ribs using surgical forceps whereby their tip hung into the opening of the aCM and were then automatically inserted for 15.5 mm with an insertion speed of 0.4 mm/s. For group 2, the aCM was filled with saline followed by application of viscose, non-crosslinked alginate-cell solution through a curved hollow needle, which thereby partly displaced the saline. Finally uncoated arrays were inserted. In group 3, the aCM was filled with saline and alginate-cell-coated arrays were inserted. To remove any detached coating, the aCM was flushed and refilled with saline after each insertion of a coated array.

2.9. Thickness of coating and classification of abrasion/delamination

Each part of the coated arrays was documented by sectionwise photographing. Arrays were fixed with their wing upright, to enable comparable positioning and orientation in the pictures. Pictures were taken with a digital color camera (Olympus XC30, Hamburg, Germany) connected to an inverse microscope (Olympus CKX 41, Hamburg,

Table 3
Grades of abrasion of coated arrays.

Grade	Abrasion of coating
0	no abrasion
1	minimal abrasion on max. ½ of array
2	minimal abrasion on > ½ of array
3	moderate abrasion on max. ½ of array
4	moderate abrasion on > ½ of array
5	severe to complete abrasion

Germany) using the 1.25-objectiv. Subsequently pictures were merged (Adobe Photoshop CS5) to depict the entire array. All coated arrays were documented at the end of the coating procedure, after the first insertion into the aCM, investigating the influence of a single insertion (comparable to the surgical procedure in patients) and after the third insertion for worst-case evaluation. The thickness of the coating was analyzed on pictures taken before the first insertion using Cell-D software (Olympus Life Science, Waltham, USA). The thickness above and below the array at the basal (Fig. 4, A) and apical (tip; Fig. 4, B) 3 mm of the carrier was measured between the surfaces of the array and the outermost alginate layer (Fig. 4, red lines) and data were averaged. Hereby a possible inhomogeneity of the coating based on alginate rinsing downwards to the tip of the array could be documented.

For the classification of the coating-stability after insertion, the merged photographs (Fig. 3, B) of the coated electrode arrays were assessed by three persons and results were averaged. The abrasion of the coating was classified in six different grades (Table 3).

3. Results

3.1. Insertion forces

The arrays in group 1 (reference group: aCM filled with saline) and group 2 (lubricant group: alginate-cell solution as lubricant for insertion in about 70% (26 mm^3) of basal turn of the aCM) showed

Table 2
Experimental groups.

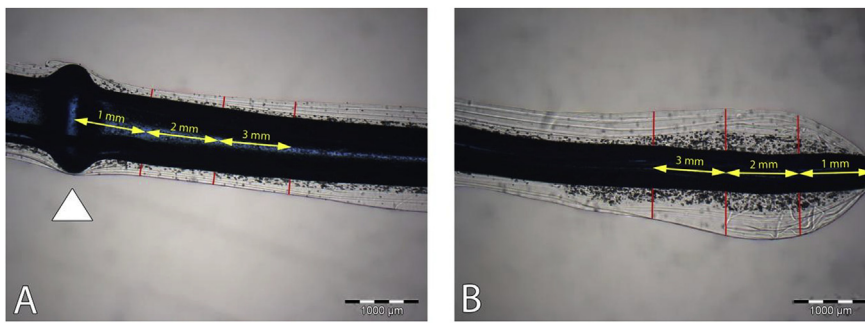|	Cochlea model filling	Electrode array coating	Sample size
Group 1: Reference	saline	no	20
Group 2: Lubricant	saline + non-crosslinked alginate encapsulated cells	no	20
Group 3: Coating	saline	crosslinked alginate encapsulated cells	20

Fig. 4. Light microscopic image of the coated basal part (**A**) and the tip (**B**). Coating thickness is measured at the basal and apical 3 mm (yellow). Thickness is measured at these three points as distance (red line) between the surface of the array to the surface of the outmost alginate layer above and below the array. Triangle points at the marker rib at the basal part of the array. Scale bar: 1000 μm.
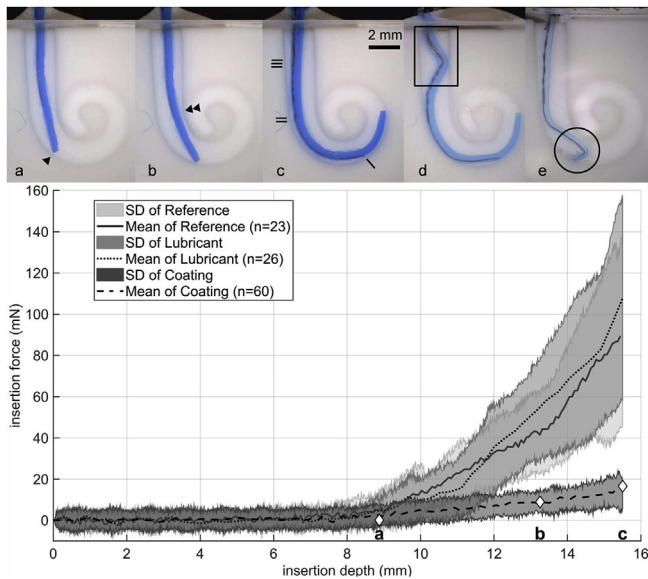

Fig. 5. Exemplarily shown insertion of a coated electrode array into the aCM (**a-c**). The first contact between the array and the aCM occurs at its outer wall (◄). The second contact occurs at the inner wall of the aCM (◄◄), after which point the array bends to follow the curved path of the aCM. Final insertion position, with marked ending of the first (−), the second (=) and the last two (≡) embedded copper wires. Occurrences of buckling (rectangle in **d**) and tip fold over (circle in **e**) are shown for completeness. Insertion forces of all three investigated groups as function of insertion depth and their standard deviations (SD). Positions (a), (b) and (c) within the insertion force diagram correspond to the small images above.

considerable occurrences of buckling and tip fold-over. In such case the movement was stopped leading to an incomplete insertion and corresponding force measurements were excluded from evaluation, resulting in 23, respectively 26, analysed insertions. Group 3 (coated arrays) showed neither buckling nor tip fold-over, so that all 60 insertions were successful and included in analysis.

Analysis was performed with data of successful (without tip fold over or buckling) and complete (from tip to marker ribs) insertions (Fig. 5). The maximal forces occurred at the very end of the insertion process (15.5 mm) and tended to be lower in the reference group (92.9 ± 46.6 mN) than in the lubricant group (107.8 ± 49.0 mN) (Figs. 5 and 6). Lowest forces at the very end of the insertion were measured for coated arrays with 12.6 ± 6.5 mN (Fig. 5). Compared to the other groups, maximal insertion forces of the coated arrays occur earlier during insertion, at an insertion depth of only 15.39 ± 0.02 mm. At this section forces of 15.4 ± 8.5 mN were achieved. Due to the observed abrasion of the coating in some arrays, the maximal insertion forces were evaluated again, differentiated for the first and the third insertion of the arrays. The mean overall maximal insertion forces, regardless of the occurring position, for the first insertion of the coated arrays was found to be 23.3 ± 8.2 mN, and

22.9 ± 7.5 mN for the third insertion (difference not significant, Mann-Whitney-U-Test, α = 0.05; Fig. 6).

Comparing the maximal insertion forces of the reference group to those of the alginate coated arrays a significant reduction of 75.2% (Mann-Whitney-U-Test, α = 0.001) can be shown (Fig. 6, A). As there is no relevant difference in maximal forces of first and third insertion of the coated arrays (Fig. 6, B), the partly observed abrasion of the coating does not seem to have an impact on insertion force.

3.2. Coating procedure, mechanical robustness and wettability

A coating mediated by pLL with pure UHV-alginate as well as with UHV-alginate encapsulated cells in layers was applicable to platinum, silicone and human-size custom-made electrode arrays. The coating was generally homogenous and a smooth surface was formed. *In vitro*, the layered coating was stable in medium for the observed three weeks and the embedded cells still expressed the fluorescent marker gene. Due to the manual dip coating procedure, there was a variability in the thickness of the applied alginate layers on the wires (Fig. 2, A) and also of the coating of the electrode arrays. The analyzed basal part had a mean thickness of 0.12 mm varying between 0.01 and 0.35 mm with no differences observed within the analyzed array length. For the apical part of the coated arrays an averaged thickness of 0.22 mm above and below the array was measured with no difference within the 3 mm analyzed. The apical coating thickness varied between 0.03 and 0.85 mm. Overall the coating was thinner on the basal part compared to the apical part, due to varying degree of droplet formation on the array-tip.

Occasionally some loose fragments of the outermost alginate layer were seen after final linkage. Nevertheless, the coating on the arrays was robust and flexible enough for the insertion procedure including a positioning of the tip within the opening of the aCM using forceps. Even a gentle straightening of bended coated array-tips by forceps after insertion for a correct positioning for the next insertion was possible without a visible abrasion of the coating.

After the first insertion, no coated array was classified to grade 5 with severe or complete abrasion of the coating (Fig. 7, A). 85% (17 out of 20) of the analyzed arrays had no to minimal signs of coating abrasion (grade 0–1). The remaining 15% (3 out of 20) were equally distributed to grade 2 to 4. In contrast, after the third insertion a reduction of the coating stability was detectable (Fig. 7, B). 40% (8 out of 20) of the coated arrays were rated to grade 5 and 4 and the number of arrays having a coating still remaining intact or nearly intact (grade 0–1) was reduced to 50% (10 out of 20). 5% (1 out of 20) of the coated arrays were classified to grade 2 and 3 each. During evaluation of the degree of abrasion, there was no visible interrelation between coating thickness and impact of abrasion detectable.

Materials with water contact angles of < 90° are classified as hydrophilic with a high wettability, while contact angles of > 90° correspond to hydrophobic surfaces with a low wettability (Bracco and Holst, 2013). Both bare silicone disks (representing the silicone surface of uncoated electrode arrays) were clearly hydrophobic with water
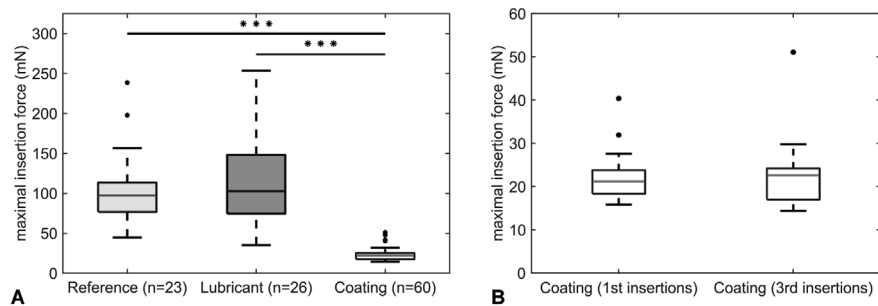
Fig. 6. Maximal insertion forces. The difference between forces of reference and lubricant group to coated group was significant (Mann-Whitney-U-Test, $\alpha = 0.001$). The mean insertion force of the reference did not differ significantly from that of the lubricant group (**A**). Insertions forces for first (median 21.4 mN) and third insertion (median 22.6 mN) of coated arrays showed no significant difference (**B**).

contact angles of $115.2° \pm 1.8°$ (clear silicone) and $116.2° \pm 0.8°$ (dyed silicone). In contrast, the alginate-coating of silicone and cover glass had a highly hydrophilic effect. The droplet for contact angle measurement immediately spread on both coated materials, after rinsing with deionized water as well. No droplet was formed for angle measurements (0°, complete wetting).

4. Discussion

In this study, two UHV-alginate-cell-based drug delivery strategies were tested for their feasibility to improve CI therapy. Using a human-sized aCM, their applicability and their influence on the insertion forces into the model were tested.

The experimental setup with custom-made electrode arrays and saline filled aCM can mimic a CI-insertion surgery only to a limited extent. For example the friction conditions while inserting an electrode array into a living cochlea may differ from the conditions of an aCM filled with an artificial fluid. Previously we were able to show that filling the aCM with saline shows very good correspondence of insertion forces when compared to fresh porcine specimen (Salcher et al., 2019). Therefore, we can state that the aCM used in the present study is an adequate artificial model for the human cochlea. The custom-made electrode arrays used within the study are straight arrays with dimensions similar to those of commercially used ones (see Table 1). With the Slim Straight (0.6–0.3 mm diameter; Cochlear Ltd.) and the Evo array (0.5–0.4 mm; Oticon Medical), only two straight electrode arrays are considerably smaller in diameter than the custom-made ones used in this study.

UHV-alginate as hydrogel matrix was chosen because of its above-mentioned desirable characteristics for an application in the inner ear. The $BaCl_2$-crosslinked UHV-alginate can tie encapsulated drug-producing cells for long-term drug delivery and shield them against the host immune system. The biocompatibility and high stability of crosslinked alginate *in vivo* has been demonstrated in several studies (e.g. (Elliott et al., 2007; Skinner et al., 2009; Wise et al., 2011; Zimmermann et al., 2005)). Additionally cells encapsulated in alginate can be protected against shear stress (Aguado et al., 2012; Foster et al., 2017), which is advantageous since high shear stress during an application of cells can damage the cell membrane and result in decreased cell survival. Thus,
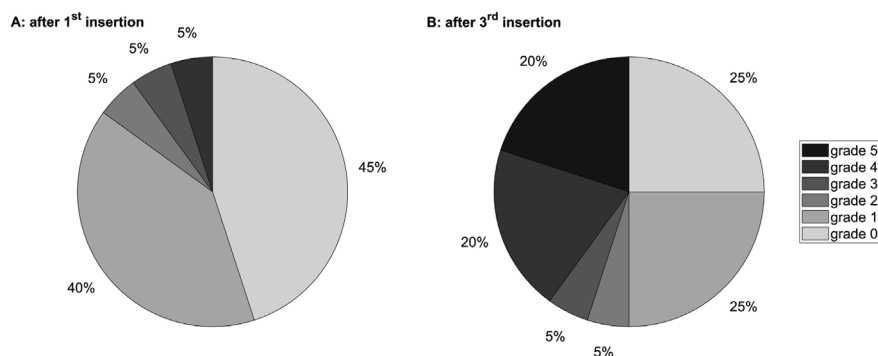
we assume a better protection of the encapsulated cells during insertion but did not focus on cell viability in the presented study. When applied as coating, the alginate creates a flexible, mechanically soft surface and shields the hydrophobic silicone of the CI-electrode (Abidian and Martin, 2009; Kim et al., 2010).

A supply of viscose alginate-cell solution for application to the inner ear could be easily included during surgical procedure and has the potential for CI improvement. Senn et al. (2017) were able to proof the concept of a gapless interface for the CI in an animal model. Neurites were regenerated under NTF-treatment through an injected functionalized gel-nanomatrix for structural support in the scala tympani. In the here presented study, we modified Senns approach of using hydrogel-injection for neurite outgrowth towards the CI onto a cell-based drug delivery system. We could proof the possibility to encapsulate NTF-producing cells in medical grade alginate under sterile conditions. Within approximately 30 min cells were detached, encapsulated and filled into a syringe ready for inner ear injection.

The measured insertion forces within our study increased slightly, although not significantly, when arrays were inserted into the alginate-cell solution filled aCM compared to an insertion into saline (reference). This is in contrast to a significant reduction of insertion forces for 50% and 75% $BaCl_2$-crosslinked alginate we detected previously (Kontorinis et al., 2012). An explanation would be that the insertion was performed in a by the liquid $BaCl_2$ for 50% and 75% diluted and not yet cross-linked alginate. In our current study, the UHV-alginate was mixed with ~17% cell suspension and was therefore less diluted and included cells, what may have caused higher insertion forces compared to saline.

The dip coating of pLL-precoated platinum wires, silicone tubings and finally the human-size custom-made electrode array was performed manually under sterile conditions and was tested stable *in vitro* for at least three weeks. A layer-by-layer application of (four) inner cell-containing and (three) outer cell-free isolating alginate layers was possible and easy to apply. The electrode arrays were completely covered with the coating from base to tip. Because of the manual procedure, each layer was individually formed, resulting in an increased standard deviation after each coating cycle. The measured thickness of the coating at the basal part of the custom-made arrays had a mean thickness of 0.12 mm, which increased to 0.22 mm (max 0.85 mm) at the apical part. The coating of our arrays increased its volume by

Fig. 7. (**A**) Coating stability after first insertion. 85% of the tested electrode arrays had no or only minimal signs of coating abrasion (grade 0–1). (**B**) When insertion into the aCM was repeated, the impact on the coating and therefore the abrasion was increased. 50% of the arrays were classified to higher grades (2–5) of abrasion after the third insertion, while 50% still had no or only minimal signs of coating abrasion (grade 0–1) (**B**). N = 20.

approximately 20%. This has to be considered for implantation surgery e.g. in term of intra cochlear pressure increase and perilymph displacement (Mittmann et al., 2017; Roland, 2005). Since there was no high deviation in the insertion forces between arrays with varying coating thicknesses and no distinct difference for the first compared to the third insertion, it is assumed that also a much thinner coating might be valuable for the advantageous force reduction. The observed droplet formation at the apical tip of the array during manual dip coating could additionally reduce the potential for insertion trauma by distribution of insertion forces (Bhatti et al., 2015). Although the thickness of our alginate coating varied widely due to the manual dip coating procedure and the coating was partly rubbed off some arrays, none of the coated arrays showed buckling or tip fold-over during insertion, while both occurred in the groups without coating. This indicates that an alginate coating (independent of its thickness) might have the potential to reduce the incidence of buckling and tip fold-over. Reasons for this could be a reduction of the friction on the cochlea wall and the modiolus, a function as mechanical buffer, the named better distribution of insertion forces and a stabilization of a soft tip without a critical impact on the flexibility.

A mostly homogenous coating with a smooth surface was applicable by the described dip coating procedure. Rarely some loose parts of the outermost alginate layer were seen without any detectable negative influence on the insertion. However, a proper adherence to the array and a high level of flexibility, a prerequisite for insertion, were achieved like requested in Schendzielorz et al., (2014).

The stability of the here presented coating was good at initial but decreased with repeated insertions. There was no visible indication that the different thicknesses of the applied coating had an influence on the stability during insertion. After the first insertion, comparable with CI-electrode implantation surgery in patients, 15% showed signs of minimal or moderate abrasion of the coating. This good stability of the coating decreased with repeated insertions. After the third insertion half of the coated arrays had an (nearly) intact coating, while one fifth showed severe delamination of the coating. In a previous study we documented a removal of CI-electrode-covering fibroblasts from the outer electrode surface after first insertion into a cochlea model but no increased removal after five repeated insertions (Kontorinis et al., 2012). We hypothesized that this result might be due to a complete detachment of all formally attached cells contacting the outer wall during first insertion into the model. In comparison, the here tested coating is composed of several layers for more stability and especially to avoid a detachment and migration of cells. But the careful straightening of bent arrays by forceps for a correct insertion, the repeated insertions and the handling for photo documentation may have had negative impact on the stability of the alginate-coating in comparison to studies presenting a complete stability of coatings (Hassarati et al., 2014; Schendzielorz et al., 2014). For insertion surgery of an alginate-cell-coated CI a more stable adherence of the tested coating is expected due to less handling. A further improvement of the coating stability could possibly be achieved by: a reduction of applied layers (requiring an increased number of encapsulated cells at the same time) or a functionalization of the interface between the single layers (Ehrhart et al., 2013) or the incorporation of microfibers into the hydrogel or the usage of a stiffer UHV-alginate (e.g. "high-G″ alginates, composed of more guluronic acid units or an increased time of final crosslinkage, with consideration of a negative influence on cell viability). Otherwise the presented results prove already a relatively good robustness of this simple and gentle cell encapsulating coating, even against handling with surgical instruments since there was no severe impact on most coated electrodes after straightening and positioning by forceps especially after the first insertion. Nevertheless, *in vivo* studies proved a good stability for implanted cells encapsulated in hydrogel, especially in UHV-alginate, for example for 6 months (Skinner et al., 2009; Wise et al., 2011) to 9.5 years (Elliott et al., 2007). Therefore, an abrasion of the coating with the encapsulated cells does not necessarily induce a

decrease in safety or biocompatibility of this cell-based drug delivery systems in contrast to cell-seeded implants without a coverage of the cells (Kontorinis et al., 2012; Roemer et al., 2016; Schendzielorz et al., 2018; Warnecke et al., 2012).

The impact of the alginate-cell coating on the insertion forces was tested in an aCM. In previous studies inconsistent results are reported for insertion forces of coated electrodes ranging from no difference (fibrin glue coating) (Roemer et al., 2016) over a slight but not significant increase (collagen and fibrin coating) (Schendzielorz et al., 2014) to an significant increase (star-shaped polyethylene glycol prepolymer-hydrogel coating of electrode array equivalent implants (optical fibres)) (Wrzeszcz et al., 2015). These results reinforce the position of the authors, whereby an assessment of a coating for drug delivery purposes based only on pharmacological aspects, like drug elution rate, is not sufficient to assess the feasibility of such a coating for clinical application since the mechanical implantability may be negatively affected (as stated in Wrzeszcz et al., 2015).

A coating of electrodes with fibroblasts halved the insertion forces compared to uncoated electrodes, whereby the cells were rubbed off the electrode during insertion (Kontorinis et al., 2012). There was no increase in forces when reinserting the partially cell-covered arrays, maybe due to remaining cells at the outer wall of the cochlea model facilitating further insertions. In the here presented study the aCM was flushed after each insertion of the coated array to exclude influences of detached alginate on the forces of following insertions. There was no difference in the measured insertion forces between first and following insertions of the same array, even when the coating was partly rubbed off. Therefore, it can be assumed that the reduction in the forces is a direct effect of the alginate coating, regardless of the coating thickness. A slight but not significant decrease of insertion forces for polydopamine-cell coated electrodes with a few detached cells during insertion as well was documented by Schendzielorz et al. (2018). Another study analyzed the impact of a flexible, biodegradable coating based of hydroxyl-ethyl-cellulose applied to prototype arrays on the insertion forces into a cochlea model (Radeloff et al., 2009). A significant average reduction of forces exceeding 50% compared to uncoated arrays was verified. Additionally, a less erratic and therefore smoother insertion into the model was detected for the coated arrays. In contrast buckling was frequently seen in the group of uncoated arrays, which both is in accordance with our results.

We assume that our detected reduction of the insertion forces and smoother insertion into the artificial cochlea model is mainly based on the hydrophilic character of the tested alginate-coating. A water contact angle of about 0° for the alginate coated surfaces compared to contact angles of $115.2° \pm 1.8°$ (clear silicone) and $116.2° \pm 0.8°$ (dyed silicone) for the uncoated silicone samples indicates the massive increase of hydrophilicity by the alginate-coating. Some disadvantages of silicone as material for CI electrodes are the native hydrophobicity, high friction and a bacterial and protein adhesive tendency (Kinoshita et al., 2015). Some *in vivo* studies showed that a hydrophilic coating of electrodes caused a better implantability, lower fibrous tissue formation and protection of hair cells and SGN (Kikkawa et al., 2014; Kinoshita et al., 2015). This was attributed to a reduction of insertion trauma during surgery. Both studies did not detect insertion forces. But one can speculate about an association between hydrophilic coatings of the silicone electrodes, our detected reduced insertion forces and a reduction of insertion trauma with a protection of hair cells and SGN. Therefore, we assume that the here presented hydrophilic UHV-alginate coating of the electrode array with the purpose of chronic endogenous cell-based drug delivery may have additional beneficial effects for the CI outcome by reducing surgically-induced trauma, foreign body reaction and protecting inner ear tissue and residual hearing.

5. Conclusions

Alginate filling of the scala tympani might be an option to bridge the

distance between the electrode contact and the regenerating peripheral dendrites of the spiral ganglion neurons and provide the necessary extracellular matrix to guide the dendrites towards the electrode contact following the gradient of NTFs secreted from the coated electrode. But changes in the scala tympani fluids and the detected higher insertion forces would limit this drug delivery system to patients without residual hearing. In contrast, the presented results of the alginate-cell-coated CI-electrodes indicate feasibility, especially for patients with residual hearing, combining the potential for long-term local drug delivery with an eminent reduction of the insertion forces. Therefore, this electrode array functionalization is a very promising candidate as drug delivery system for inner ear therapy with an expected reduced trauma during CI surgery and a high potential for improvement of hearing outcome. Beside drug delivery, the results also open up new opportunities for application of a pure alginate coating to positively influence implantation behavior of CI-electrodes by reduction of insertion forces.

This study detected forces in an aCM, which can mimic the forces of a CI inserted into a living cochlea only to a limited intent. Therefore, human temporal bone studies and preclinical *in vivo* studies should be performed to give a deeper insight into a reduction of the forces and a protection of the delicate intracochlear structures during insertion of an alginate-cell-coated CI. Further investigations have to focus on an additional improvement of the uniformity of the coating and the stability during insertion. Also the effects of coated electrodes with and without cells regarding intracochlear pressure, impedance changes and safe charge delivery capabilities have to be examined.

Declarations of interest

None.

Appendix A. Supplementary data

Supplementary data to this article can be found online at https://doi.org/10.1016/j.jmbbm.2019.05.007.

References

Abidian, M.R., Martin, D.C., 2009. Multifunctional nanobiomaterials for neural interfaces. Adv. Funct. Mater. 19, 573–585. https://doi.org/10.1002/adfm.200801473.

Aguado, B.A., Mulyasasmita, W., Su, J., Lampe, K.J., Heilshorn, S.C., 2012. Improving viability of stem cells during syringe needle flow through the design of hydrogel cell carriers. Tissue Eng. 18, 806–815. https://doi.org/10.1089/ten.tea.2011.0391.

Bajpai, S.K., Sharma, S., 2004. Investigation of swelling/degradation behaviour of alginate beads crosslinked with Ca2 + and Ba2 + ions. React. Funct. Polym. 59, 129–140. https://doi.org/10.1016/j.reactfunctpolym.2004.01.002.

Bas, E., Dinh, C.T., Garnham, C., Polak, M., Van de Water, T.R., 2012. Conservation of hearing and protection of hair cells in cochlear implant patients' with residual hearing. Anat. Rec. Adv. Integr. Anat. Evol. Biol. 295, 1909–1927. https://doi.org/10.1002/ar.22574.

Bas, E., Goncalves, S., Adams, M., Dinh, C.T., Bas, J.M., Van De Water, T.R., Eshraghi, A.A., 2015. Spiral ganglion cells and macrophages initiate neuro-inflammation and scarring following cochlear implantation. Front. Cell. Neurosci. 9. https://doi.org/10.3389/fncel.2015.00303.

Bhatti, P., Van Beek-King, J., Sharpe, A., Crawford, J., Tridandapani, S., McKinnon, B., Blake, D., 2015. Highly flexible silicone coated neural array for intracochlear electrical stimulation. BioMed Res. Int. 2015, 1–10. https://doi.org/10.1155/2015/109702.

Bohl, A., Rohm, H.W., Ceschi, P., Paasche, G., Hahn, A., Barcikowski, S., Lenarz, T., Stöver, T., Pau, H.-W., Schmitz, K.-P., Sternberg, K., 2012. Development of a specially tailored local drug delivery system for the prevention of fibrosis after insertion of cochlear implants into the inner ear. J. Mater. Sci. Mater. Med. 23, 2151–2162.

https://doi.org/10.1007/s10856-012-4698-z.

Bracco, G., Holst, B., 2013. Surface Science Techniques, Springer Series in Surface Sciences, Springer Series in Surface Sciences. Springer Berlin Heidelberg, Berlin, Heidelberg. https://doi.org/10.1007/978-3-642-34243-1.

Ceschi, P., Bohl, A., Sternberg, K., Neumeister, A., Senz, V., Schmitz, K.P., Kietzmann, M., Scheper, V., Lenarz, T., Stöver, T., Paasche, G., 2014. Biodegradable polymeric coatings on cochlear implant surfaces and their influence on spiral ganglion cell survival. J. Biomed. Mater. Res. B Appl. Biomater. 102, 1255–1267. https://doi.org/10.1002/jbm.b.33110.

De Vos, P., De Haan, B., Van Schilfgaarde, R., 1997. Effect of the alginate composition on the biocompatibility of alginate-polylysine microcapsules. Biomaterials 18, 273–278.

Dhanasingh, A., Jolly, C., 2017. An overview of cochlear implant electrode array designs. Hear. Res. 356, 93–103. https://doi.org/10.1016/j.heares.2017.10.005.

Drouillard, M., Torres, R., Mamelle, E., De Seta, D., Sterkers, O., Ferrary, E., Nguyen, Y., 2017. Influence of electrode array stiffness and diameter on hearing in cochlear implanted Guinea pig. PLoS One 12, e0183674. https://doi.org/10.1371/journal.pone.0183674.

Ehrhart, F., Mettler, E., Böse, T., Weber, M.M., Vásquez, J.A., Zimmermann, H., 2013. Biocompatible coating of encapsulated cells using ionotropic gelation. PLoS One 8, e73498. https://doi.org/10.1371/journal.pone.0073498.

Elliott, R.B., Escobar, L., Tan, P.L.J., Muzina, M., Zwain, S., Buchanan, C., 2007. Live encapsulated porcine islets from a type 1 diabetic patient 9.5 yr after xenotransplantation. Xenotransplantation 14, 157–161. https://doi.org/10.1111/j.1399-3089.2007.00384.x.

Farhadi, M., Jalessi, M., Salehian, P., Ghavi, F.F., Emamjomeh, H., Mirzadeh, H., Imani, M., Jolly, C., 2013. Dexamethasone eluting cochlear implant: histological study in animal model. Cochlear Implants Int. 14, 45–50. https://doi.org/10.1179/1754762811Y.0000000024.

Foster, A.A., Marquardt, L.M., Heilshorn, S.C., 2017. The diverse roles of hydrogel mechanics in injectable stem cell transplantation. Curr. Opin. Chem. Eng. 15, 15–23. https://doi.org/10.1016/j.coche.2016.11.003.

Gepp, M., Ehrhart, F., Shirley, S., Howitz, S., Zimmermann, H., 2009. Dispensing of very low volumes of ultra high viscosity alginate gels: a new tool for encapsulation of adherent cells and rapid prototyping of scaffolds and implants. Biotechniques 46, 31–43. https://doi.org/10.2144/000113014.

Gillespie, L.N., Clark, G.M., Bartlett, P.F., Marzella, P.L., 2003. BDNF-induced survival of auditory neurons in vivo: cessation of treatment leads to accelerated loss of survival effects. J. Neurosci. Res. 71, 785–790. https://doi.org/10.1002/jnr.10542.

Gillespie, L.N., Richardson, R.T., Nayagam, B.A., Wise, A.K., 2014. Treating hearing disorders with cell and gene therapy. J. Neural Eng. 11, 065001. https://doi.org/10.1088/1741-2560/11/6/065001.

Gillespie, L.N., Shepherd, R.K., 2005. Clinical application of neurotrophic factors: the potential for primary auditory neuron protection. Eur. J. Neurosci. 22, 2123–2133. https://doi.org/10.1111/j.1460-9568.2005.04430.x.

Glueckert, R., Bitsche, M., Miller, J.M., Zhu, Y., Prieskorn, D.M., Altschuler, R.A., Schrott-Fischer, A., 2008. Deafferentiation-associated changes in afferent and efferent processes in the Guinea pig cochlea and afferent regeneration with chronic intrascalar brain-derived neurotrophic factor and acidic fibroblast growth factor. J. Comp. Neurol. 507, 1602–1621. https://doi.org/10.1002/cne.21619.

Glueckert, R., Pfaller, K., Kinnefors, A., Rask-Andersen, H., Schrott-Fischer, A., 2005. The human spiral ganglion: new insights into ultrastructure, survival rate and implications for cochlear implants. Audiol. Neurotol. 10, 258–273. https://doi.org/10.1159/000086000.

Gnansia, D., Demarcy, T., Vandersteen, C., Raffaelli, C., Guevara, N., Delingette, H., Ayache, N., 2016. Optimal electrode diameter in relation to volume of the cochlea. Eur. Ann. Otorhinolaryngol. Head Neck Dis. 133, S66–S67. https://doi.org/10.1016/j.anorl.2016.04.013.

Harper, M.M., Grozdanic, S.D., Blits, B., Kuehn, M.H., Zamzow, D., Buss, J.E., Kardon, R.H., Sakaguchi, D.S., 2011. Transplantation of BDNF-secreting mesenchymal stem cells provides neuroprotection in chronically hypertensive rat eyes. Investig. Opthalmology Vis. Sci. 52, 4506. https://doi.org/10.1167/iovs.11-7346.

Hassarati, R.T., Dueck, W.F., Tasche, C., Carter, P.M., Poole-Warren, L.A., Green, R.A., 2014. Improving cochlear implant properties through conductive hydrogel coatings. IEEE Trans. Neural Syst. Rehabil. Eng. 22, 411–418. https://doi.org/10.1109/TNSRE.2014.2304559.

Hügl, S., Rülander, K., Lenarz, T., Majdani, O., Rau, T.S., 2018. Investigation of ultra-low insertion speeds in an inelastic artificial cochlear model using custom-made cochlear implant electrodes. Eur. Arch. Oto-Rhino-Laryngol. 275, 2947–2956. https://doi.org/10.1007/s00405-018-5159-1.

Hütten, M., Erhacrt, F., Zimmermann, H., Reich, U., Esser, K.-H., Lenarz, T., Scheper, V., 2013. UHV-alginate as matrix for neurotrophic factor producing cells—a novel biomaterial for cochlear implant optimization to preserve inner ear neurons from degeneration. Otol. Neurotol. 34, 1127–1133. https://doi.org/10.1097/MAO.0b013e3182804949.

Kikkawa, Y.S., Nakagawa, T., Ying, L., Tabata, Y., Tsubouchi, H., Ido, A., Ito, J., 2014. Growth factor-eluting cochlear implant electrode: impact on residual auditory function, insertional trauma, and fibrosis. J. Transl. Med. 12, 280. https://doi.org/10.1186/s12967-014-0280-4.

Kim, D.-H., Wiler, J.A., Anderson, D.J., Kipke, D.R., Martin, D.C., 2010. Conducting polymers on hydrogel-coated neural electrode provide sensitive neural recordings in auditory cortex. Acta Biomater. 6, 57–62. https://doi.org/10.1016/j.actbio.2009.07.034.

Kinoshita, M., Kikkawa, Y.S., Sakamoto, T., Kondo, K., Ishihara, K., Konno, T., Pawsey, N., Yamasoba, T., 2015. Safety, reliability, and operability of cochlear implant electrode arrays coated with biocompatible polymer. Acta Otolaryngol. 135, 320–327. https://doi.org/10.3109/00016489.2014.990580.

Konerding, W.S., Janssen, H., Hubka, P., Tornøe, J., Mistrik, P., Wahlberg, L., Lenarz, T., Kral, A., Scheper, V., 2017. Encapsulated cell device approach for combined electrical stimulation and neurotrophic treatment of the deaf cochlea. Hear. Res. 350, 110–121. https://doi.org/10.1016/j.heares.2017.04.013.

Kontorinis, G., Paasche, G., Lenarz, T., Stöver, T., 2011. The effect of different lubricants on cochlear implant electrode insertion forces. Otol. Neurotol. 32, 1050–1056. https://doi.org/10.1097/MAO.0b013e31821b3c88.

Kontorinis, G., Scheper, V., Wissel, K., Stöver, T., Lenarz, T., Paasche, G., 2012. In vitro modifications of the scala tympani environment and the cochlear implant array surface. Laryngoscope 122, 2057–2063. https://doi.org/10.1002/lary.23408.

Landry, T.G., Fallon, J.B., Wise, A.K., Shepherd, R.K., 2013. Chronic neurotrophin delivery promotes ectopic neurite growth from the spiral ganglion of deafened cochleae without compromising the spatial selectivity of cochlear implants. J. Comp. Neurol. 521, 2818–2832. https://doi.org/10.1002/cne.23318.

Lehnhardt, E., 1993. [Intracochlear placement of cochlear implant electrodes in soft surgery technique]. HNO 41, 356–359.

Lenarz, T., Stöver, T., Buechner, A., Lesinski-Schiedat, A., Patrick, J., Pesch, J., 2009. Hearing conservation surgery using the hybrid-L electrode. Audiol. Neurotol. 14, 22–31. https://doi.org/10.1159/000206492.

Leon, L., Warren, F.M., Abbott, J.J., 2018. An in-vitro insertion-force study of magnetically guided lateral-wall cochlear-implant electrode arrays. Otol. Neurotol. 39, e63–e73. https://doi.org/10.1097/MAO.0000000000001647.

Liu, H., Hao, J., Li, K.S., 2013. Current strategies for drug delivery to the inner ear. Acta Pharm. Sin. B 3, 86–96. https://doi.org/10.1016/j.apsb.2013.02.003.

Mistrík, P., Jolly, C., Sieber, D., Hochmair, I., 2017. Challenging aspects of contemporary cochlear implant electrode array design. World J. Otorhinolaryngol. - Head Neck Surg. 3, 192–199. https://doi.org/10.1016/j.wjorl.2017.12.007.

Mittmann, P., Mittmann, M., Ernst, A., Todt, I., 2017. Intracochlear pressure changes due to 2 electrode types: an artificial model experiment. Otolaryngol. Neck Surg. 156, 712–716. https://doi.org/10.1177/0194599816684104.

Mom, T., Bachy, A., Houette, A., Pavier, Y., Pastourel, R., Gabrillargues, J., Saroul, N., Gilain, L., Avan, P., 2016. Cochlear implantation through the round window with a straight slotted electrode array: optimizing the surgical procedure. Eur. Arch. Oto-Rhino-Laryngol. 273, 853–858. https://doi.org/10.1007/s00405-015-3623-8.

Nadol, J.B., Young, Y.-S., Glynn, R.J., 1989. Survival of spiral ganglion cells in profound sensorineural hearing loss: implications for cochlear implantation. Ann. Otol. Rhinol. Laryngol. 98, 411–416. https://doi.org/10.1177/000348948909800602.

Nguyen, Y., Miroir, M., Kazmitcheff, G., Sutter, J., Bensidhoum, M., Ferrary, E., Sterkers, O., Bozorg Grayeli, A., 2012. Cochlear implant insertion forces in microdissected human cochlea to evaluate a prototype Array. Audiol. Neurotol. 17, 290–298. https://doi.org/10.1159/000338406.

Nguyen, Y., Mosnier, I., Borel, S., Ambert-Dahan, E., Bouccara, D., Bozorg-Grayeli, A., Ferrary, E., Sterkers, O., 2013. Evolution of electrode array diameter for hearing preservation in cochlear implantation. Acta Otolaryngol. 133, 116–122. https://doi.org/10.3109/00016489.2012.723824.

Oticon medical, 2019. Electrode arrays versions product overview product overview. [WWW Document]. https://www.oticonmedical.com/-/media/medical/main/files/ci/products/neuro-zti/pi/en/neuro-zti-product-information—english—m80689.pdf?la=en (accessed 2.22.19).

Pettingill, L.N., Richardson, R.T., Wise, A.K., O'Leary, S.J., Shepherd, R.K., 2007. Neurotrophic factors and neural prostheses: potential clinical applications based upon findings in the auditory system. IEEE Trans. Biomed. Eng. 54, 1138–1148. https://doi.org/10.1109/TBME.2007.895375.

Pettingill, L.N., Wise, A.K., Geaney, M.S., Shepherd, R.K., 2011. Enhanced auditory neuron survival following cell-based BDNF treatment in the deaf Guinea pig. PLoS One 6, e18733. https://doi.org/10.1371/journal.pone.0018733.

Radeloff, A., Unkelbach, M.H., Mack, M.G., Settevendemie, C., Helbig, S., Mueller, J., Hagen, R., Mlynski, R., 2009. A coated electrode carrier for cochlear implantation reduces insertion forces. Laryngoscope 119, 959–963. https://doi.org/10.1002/lary.20206.

Rejali, D., Lee, V.A., Abrashkin, K.A., Humayun, N., Swiderski, D.L., Raphael, Y., 2007. Cochlear implants and ex vivo BDNF gene therapy protect spiral ganglion neurons. Hear. Res. 228, 180–187. https://doi.org/10.1016/j.heares.2007.02.010.

Roehm, P.C., Hansen, M.R., 2005. Strategies to preserve or regenerate spiral ganglion neurons. Curr. Opin. Otolaryngol. Head Neck Surg. 13, 294–300. https://doi.org/10.1097/01.moo.0000180919.68812.b9.

Roemer, A., Köhl, U., Majdani, O., Klöß, S., Falk, C., Haumann, S., Lenarz, T., Kral, A., Warnecke, A., 2016. Biohybrid cochlear implants in human neurosensory restoration. Stem Cell Res. Ther. 7, 148. https://doi.org/10.1186/s13287-016-0408-y.

Roland, J.T., 2005. A model for cochlear implant electrode insertion and force evaluation: results with a new electrode design and insertion technique. Laryngoscope 115, 1325–1339. https://doi.org/10.1097/01.mlg.0000167993.05007.35.

Salcher, R., Nullmeier, M., Cramer, J., Pawsey, N., Lenarz, T., Rau, T.S., 2019. Validation of PTFE artificial cochlea model for insertion force measurements. In: ARO 42nd Annual MidWinter Meeting.

Sasaki, M., Radtke, C., Tan, A.M., Zhao, P., Hamada, H., Houkin, K., Honmou, O., Kocsis, J.D., 2009. BDNF-hypersecreting human mesenchymal stem cells promote functional recovery, axonal sprouting, and protection of corticospinal neurons after spinal cord injury. J. Neurosci. 29, 14932–14941. https://doi.org/10.1523/JNEUROSCI.2769-09.2009.

Schendzielorz, P., Rak, K., Radeloff, K., Völker, J., Gehrke, T., Scherzad, A., Kleinsasser, N., Hagen, R., Radeloff, A., 2018. A polydopamine peptide coating enables adipose-derived stem cell growth on the silicone surface of cochlear implant electrode arrays. J. Biomed. Mater. Res. B Appl. Biomater. 106, 1431–1438. https://doi.org/10.1002/jbm.b.33947.

Schendzielorz, P., Scherzed, A., Rak, K., Völker, J., Hagen, R., Mlynski, R., Frölich, K., Radeloff, A., 2014. A hydrogel coating for cochlear implant arrays with encapsulated adipose-derived stem cells allows brain-derived neurotrophic factor delivery. Acta Otolaryngol. 134, 497–505. https://doi.org/10.3109/00016489.2013.878809.

Schneider, S., Feilen, P.J., Kraus, O., Haase, T., Sagban, T.A., Lehr, H., Beyer, J., Pommersheim, R., Weber, M.M., 2003. Biocompatibility of alginates for grafting:

impact of alginate molecular weight. Artif. Cells, blood substitutes. Biotechnology 31, 383–394. https://doi.org/10.1081/BIO-120025409.

Schwieger, J., Hügl, S., Hamm, A., Lenarz, T., Hoffmann, A., Rau, T., Scheper, V., 2018. BDNF-producing human mesenchymal stem cells in an alginate-matrix: neuroprotection and cochlear implant coating stability in vitro. In: Laryngo-Rhino-Otologie, 382–382. https://doi.org/10.1055/s-0038-1641059.

Schwieger, J., Warnecke, A., Lenarz, T., Esser, K.-H., Scheper, V., 2015. Neuronal survival, morphology and outgrowth of spiral ganglion neurons using a defined growth factor combination. PLoS One 10, e0133680. https://doi.org/10.1371/journal.pone.0133680.

Senn, P., Roccio, M., Hahnewald, S., Frick, C., Kwiatkowska, M., Ishikawa, M., Bako, P., Li, H., Edin, F., Liu, W., Rask-Andersen, H., Pyykkö, I., Zou, J., Mannerström, M., Keppner, H., Homsy, A., Laux, E., Llera, M., Lellouche, J.-P., Ostrovsky, S., Banin, E., Gedanken, A., Perkas, N., Wank, U., Wiesmüller, K.-H., Mistrík, P., Benav, H., Garnham, C., Jolly, C., Gander, F., Ulrich, P., Müller, A., Löwenheim, H., 2017. NANOCI—nanotechnology based cochlear implant with gapless interface to auditory neurons. Otol. Neurotol. 38, e224–e231. https://doi.org/10.1097/MAO.0000000000001439.

Seyyedi, M., Viana, L.M., Nadol, J.B., 2014. Within-subject comparison of Word recognition and spiral ganglion cell count in bilateral cochlear implant recipients. Otol. Neurotol. 35, 1. https://doi.org/10.1097/MAO.0000000000000443.

Shepherd, R.K., Coco, A., Epp, S.B., 2008. Neurotrophins and electrical stimulation for protection and repair of spiral ganglion neurons following sensorineural hearing loss. Hear. Res. 242, 100–109. https://doi.org/10.1016/j.heares.2007.12.005.

Shepherd, R.K., Coco, A., Epp, S.B., Crook, J.M., 2005. Chronic depolarization enhances the trophic effects of brain-derived neurotrophic factor in rescuing auditory neurons following a sensorineural hearing loss. J. Comp. Neurol. 486, 145–158. https://doi.org/10.1002/cne.20564.

Shibata, S.B., Cortez, S.R., Beyer, L.A., Wiler, J.A., Di Polo, A., Pfingst, B.E., Raphael, Y., 2010. Transgenic BDNF induces nerve fiber regrowth into the auditory epithelium in deaf cochleae. Exp. Neurol. 223, 464–472. https://doi.org/10.1016/j.expneurol.2010.01.011.

Skinner, S.J.M., Geaney, M.S., Lin, H., Muzina, M., Anal, A.K., Elliott, R.B., Tan, P.L.J., 2009. Encapsulated living choroid plexus cells: potential long-term treatments for central nervous system disease and trauma. J. Neural Eng. 6, 065001. https://doi.org/10.1088/1741-2560/6/6/065001.

Stevens, G., Flaxman, S., Brunskill, E., Mascarenhas, M., Mathers, C.D., Finucane, M., 2013. Global and regional hearing impairment prevalence: an analysis of 42 studies in 29 countries. Eur. J. Public Health 23, 146–152. https://doi.org/10.1093/eurpub/ckr176.

Tam, S.K., Dusseault, J., Bilodeau, S., Langlois, G., Hallé, J.-P., Yahia, L., 2011. Factors influencing alginate gel biocompatibility. J. Biomed. Mater. Res. A 98A, 40–52. https://doi.org/10.1002/jbm.a.33047.

van de Water, T.R., Dinh, C.T., Vivero, R., Hoosien, G., Eshraghi, A.A., Balkany, T.J., 2010. Mechanisms of hearing loss from trauma and inflammation: otoprotective therapies from the laboratory to the clinic. Acta Otolaryngol. 130, 308–311. https://doi.org/10.3109/00016480903124655.

Warnecke, A., Sasse, S., Wenzel, G.I., Hoffmann, A., Gross, G., Paasche, G., Scheper, V., Reich, U., Esser, K.-H., Lenarz, T., Stöver, T., Wissel, K., 2012. Stable release of BDNF from the fibroblast cell line NIH3T3 grown on silicone elastomers enhances survival of spiral ganglion cells in vitro and in vivo. Hear. Res. 289, 86–97. https://doi.org/10.1016/j.heares.2012.04.007.

Wilk, M., Hessler, R., Mugridge, K., Jolly, C., Fehr, M., Lenarz, T., Scheper, V., 2016. Impedance changes and fibrous tissue growth after cochlear implantation are correlated and can Be reduced using a dexamethasone eluting electrode. PLoS One 11, e0147552. https://doi.org/10.1371/journal.pone.0147552.

Wise, A.K., Fallon, J.B., Neil, A.J., Pettingill, L.N., Geaney, M.S., Skinner, S.J., Shepherd, R.K., 2011. Combining cell-based therapies and neural prostheses to promote neural survival. Neurotherapeutics 8, 774–787. https://doi.org/10.1007/s13311-011-0070-0.

Word Health Organization, 2018. Deafness and Hearing Loss. [WWW Document]. http://www.who.int/en/news-room/fact-sheets/detail/deafness-and-hearing-loss (accessed 11.2.18).

Wrzeszcz, A., Dittrich, B., Haamann, D., Aliuos, P., Klee, D., Nolte, I., Lenarz, T., Reuter, G., 2014. Dexamethasone released from cochlear implant coatings combined with a protein repellent hydrogel layer inhibits fibroblast proliferation. J. Biomed. Mater. Res. A 102, 442–454. https://doi.org/10.1002/jbm.a.34719.

Wrzeszcz, A., Steffens, M., Balster, S., Warnecke, A., Dittrich, B., Lenarz, T., Reuter, G., 2015. Hydrogel coated and dexamethasone releasing cochlear implants: quantification of fibrosis in Guinea pigs and evaluation of insertion forces in a human cochlea model. J. Biomed. Mater. Res. B Appl. Biomater. 103, 169–178. https://doi.org/10.1002/jbm.b.33187.

Zhao, L.-X., Zhang, J., Cao, F., Meng, L., Wang, D.-M., Li, Y.-H., Nan, X., Jiao, W.-C., Zheng, M., Xu, X.-H., Pei, X.-T., 2004. Modification of the brain-derived neurotrophic factor gene: a portal to transform mesenchymal stem cells into advantageous engineering cells for neuroregeneration and neuroprotection. Exp. Neurol. 190, 396–406. https://doi.org/10.1016/j.expneurol.2004.06.025.

Zimmermann, H., Shirley, S.G., Zimmermann, U., 2007. Alginate-based encapsulation of cells: past, present, and future. Curr. Diabetes Rep. 7, 314–320. https://doi.org/10.1007/s11892-007-0051-1.

Zimmermann, H., Zimmermann, D., Reuss, R., Feilen, P.J., Manz, B., Katsen, A., Weber, M., Ihmig, F.R., Ehrhart, F., Geßner, P., Behringer, M., Steinbach, A., Wegner, L.H., Sukhorukov, V.L., Vásquez, J.A., Schneider, S., Weber, M.M., Volke, F., Wolf, R., Zimmermann, U., 2005. Towards a medically approved technology for alginate-based microcapsules allowing long-term immunoisolated transplantation. J. Mater. Sci. Mater. Med. 16, 491–501. https://doi.org/10.1007/s10856-005-0523-2.